International Journal of Engineering

Journal Homepage: www.ije.ir

Modelling and Numerical Simulation of Cutting Stress in End Milling of Titanium Alloy using Carbide Coated Tool

B. Li[a*], Y. Wang[b], H. Li [a], H. You [a]

[a] *School of Mechanical Engineering, Luoyang Institute of Science and Technology, Luoyang 471023, Henan Province, PR China*
[b] *School of Environmental Engineering and Chemistry, Luoyang Institute of Science and Technology, Luoyang 471023, Henan Province, PR China*

PAPER INFO

Paper history:
Received 19 April 2015
Received in revised form 25 May 2015
Accepted 11 June 2015

Keywords:
Finite Element Modeling
End-milling
Cutting Force
Simulation

ABSTRACT

The mechanistic force models were introduced in high accuracy force predictions for most applications. Experiment was made for the milling of titanium alloy by coated cemented carbide cutting tool. Based on the cutting force theory, test results and finite element method, we can get the expression of resultant cutting force accurately, which can be developed to a big cutting database. According to the analysis, the maximum deformation and effective stress showed an increasing trend for the machining with end-milling cutting tool. A reasonable set of milling parameters for the machining of titanium alloy by coated cemented carbide cutting tool was obtained by analyzing the cutting efficiency in relation to cutting force of the tools. It is expected that this study would provide a fundamental basis for the optimization of the cutting parameters for titanium alloy.

***doi**: 10.5829/idosi.ije.2015.28.07a.16*

NOMENCLATURE

F_a	Axial force	P	Cutting power
F_t	Tangential force	r	Cutting ratio
F_r	Radial force	v_c	Cutting speed
F_p	Cutting forces in the cutting speed	α	Rake angle
F_q	Cutting forces in the feed direction	β	Helix angle
f_t	Force coefficients	τ	Shear stress in the shear plane
h_a	Average chip thickness	φ	Immersion angle measured from the positive y–axis
K	Milling force coefficient	ϕ_n	Shear angle in the normal plane
T	Cutting torque	η_c	Chip flow angle measured on the rake face

1. INTRODUCTION

Milling is one of the most extended cutting processes due to its wide application in automotive, aerospace, mould and die, and other industries. For more than one hundred years, modelling, simulation and control of cutting forces were the important research issues for improving the workpiece surface quality, tool wear resistance and machining stability. Nevertheless, there still exist several important aspects in milling operation that need to be studied in depth to gain better understanding of the process.

Unlike other machining processes, milling is affected by several variables. The deformations and wear of tool are characteristics that affect the milling operation. Among these characteristics, the radial tool run-out in end milling received special attention from the researchers starting from the work by Kline and DeVor [1], which focused on the effects of radial tool run out on cutting forces in end milling. Several studies were conducted on the dynamic cutting processes. But most of these studies were highly simplified and the

*Corresponding Author's Email: libinman@gmail.com (B. Li)

Please cite this article as: B. Li, Y. Wang, H. Li, H. You, Modelling and Numerical Simulation of Cutting Stress in End Milling of Titanium Alloy using Carbide Coated Tool, International Journal of Engineering (IJE), TRANSACTIONS A: Basics Vol. 28, No. 7, (July 2015) 1090-1098

over simplification of earlier models resulted in poor agreement between the simulation and experimental results, and it is more evident in low speed cutting [2]. In the earlier studies on milling dynamics, mean cutting force coefficients were used for the modeling and simulation of cutting forces [3]. This mechanistic approach was used to obtain the dynamic equations of various milling processes and to predict the deflections and form errors of the machined parts [4]. In this approach, the cutting force coefficients were obtained by the experimental data under certain cutting conditions. Alternatively, the mechanics of cutting were used for the determination of milling force coefficients. In this method, after the determination of flank forces, angles made by friction and shear force from the cutting test, and the mechanics of the milling process were used for transforming the data to oblique cutting conditions [5, 6]. Titanium and its alloys are used extensively in aerospace industry because of their excellent combination of properties of high specific strength, which is maintained even at elevated temperature, their fracture resistant characteristics, and their exceptional resistance to corrosion. Titanium milling is widely used in the aerospace industry, and is also used increasingly in military, racing and medical applications.

Modeling of milling process was studied extensively [7]. The mechanistic approach was widely used for the force predictions and also extended to predict deflections and form errors [8, 9]. An alternative method of mechanics of cutting approach was used in determining milling force coefficients [10, 11].

Another major limitation in the productivity and surface quality in milling is from chatter vibrations which developed due to dynamic interactions between the cutting tool and workpiece. The chatter vibrations result from poor surface finish and reduced tool life. Budak and Altintas [12] developed a method for analytical determination of stability limits. The stability of low radial immersion milling was investigated and a model was presented for twice the number of stability lobes. All these methods can be used to generate stability diagrams from which the stable cutting conditions, and spindle speeds resulting in much higher stability can be determined for a given work material, tool geometry and transfer functions [13-15].

The demonstration of cutting model implementation in CAD/CAM systems was shown by several researchers. Altintas and Spence [16] demonstrated that the force models could be used to predict form errors and optimize feed rates based on simulation at the CAD/CAM stage itself. Weck et al. [17] demonstrated the determination of chatter free milling conditions in a commercial CAD/CAM software. The cutting force coefficients and tool dynamics were needed for these simulations, which were determined experimentally. The generation of an orthogonal cutting database for a work material by Budak et al. [18] reduced the experimentation, and thus made implementation of force models in CAD/CAM more practical.

Currently, the selection of milling parameters of titanium alloy such as the rotating speed of machine, cutting depth, feed rate, and cutting width were mainly determined with a reference to the imported manuals for cutting tools by the engineering technicians. However, the processing parameters recommended in these manuals are applicable to some common materials. These parameters are impossible to be specially designed for the material used in an enterprise. Furthermore, it is difficult to realize the optimization of cutting parameters due to lack of sufficient empirical parameters and test data. Instead of experiences, there is a need for more optimization of the parameters with theoretical basis accurately and stably, which easily causes a situation for cost reduction with a long-term optimization. In this paper, the experiment was made for the milling of titanium alloy by coated cemented carbide cutting tool. After some cutting tests, a simple cutting database is generated for a certain tool and titanium alloy materials. The mechanistic force models were introduced in high accuracy force predictions for applications. Based on the cutting force theory, previous test results and finite element method, we can get the expression of resultant cutting force accurately, which can be developed to a big cutting database. According to it, reasonable cutting parameters of the processing of titanium alloy can be obtained by the analysis of the cutting efficiency versus cutting force of the tools.

2. MODELLING OF END MILLING FORCES

A schematic description of these models is outlined in Figure 1, where φ is the immersion angle measured from the positive y–axis, the axial force component. F_a, is in the axial direct ion of the cutting tool, which is perpendicular to the cross-section shown in Figure 1.

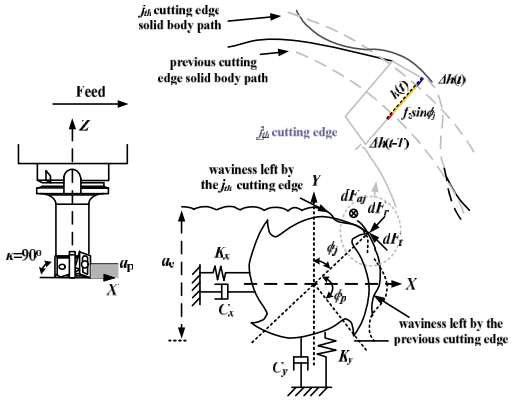

Figure 1. Schematic diagram of a model of milling

Milling forces can be modeled for given cutter geometry, cutting conditions, and work material. For evaluating a spindle in working conditions it is necessary to have a model of the process where the cutting parameters, the workpiece material properties and the tool geometry are involved.

Models follow the following steps: (*a*) the relation between the chip thickness and the vibration of the system must be formulated; (*b*) a cutting forces model is proposed; (*c*) the system dynamics is introduced, and finally (*d*) the problem that defines the stability of the process is solved. For a point on the(j^{th}) cutting tooth, differential milling forces corresponding to an infinitesimal element thickness(dz) in the tangential, dF_t, radial, dF_r , and axial, dF_a, directions can be given as:

$$\begin{aligned} \mathrm{dF}_{tj}(\phi,z) &= K_t h_j(\phi,z)dz \\ \mathrm{dF}_{rj}(\phi,z) &= K_r dF_{tj}(\phi,z) \\ \mathrm{dF}_{aj}(\phi,z) &= K_a dF_{tj}(\phi,z) \end{aligned} \quad (1)$$

In Equation (1), the edge forces are also included in the cutting force coefficient which is usually referred to as the exponential force model. They are separated from the cutting force coefficients in edge force or liner-edge force model [19]:

$$\begin{aligned} \mathrm{dF}_{tj}(\phi,z) &= [K_{te} + K_{tc} h_j(\phi,z)]dz \\ \mathrm{dF}_{rj}(\phi,z) &= [K_{re} + K_{rc} h_j(\phi,z)]dz \\ \mathrm{dF}_{aj}(\phi,z) &= [K_{ae} + K_{ac} h_j(\phi,z)]dz \end{aligned} \quad (2)$$

In Equation (2), the radial (w) and axial depth of cut (a), number of teeth (N), cutter radius (R) and helix angle (β) determine what portion of a tooth is in contact with the work piece for a given angular orientation of the cutter. $\phi = \Omega t$, where t is the time, Ω is the angular speed in (rad/s) or $\Omega = 2\pi n/60$, n being the rpm of the spindle. The chip thickness at a certain location on the cutting edge can be approximated as follows:

$$h_j(\phi,z) = f_t \sin\phi_j(\mathrm{z}) \quad (3)$$

where f_t is the feed per tooth and $\phi_j(z)$ is the immersion angle for the flute (j) at axial position z. Due to the helical flute, the immersion angle changes along the axial direction as follows:

$$\phi_j(\mathrm{z}) = \phi + (j-1)\phi_P - \frac{\tan\beta}{R} z \quad (4)$$

In Equation (4), the pitch angle is defined as $\phi_P = 2\pi/\mathrm{N}$. The tangential, radial and axial forces given by Equation (1) and (2) can be resolved in the feed, x, normal, y, and the axial direction, z, and can be integrated within the immersed part of the tool to obtain the total milling forces applied on each tooth. For the exponential force model, the following is obtained after the integration [20]:

$$\begin{aligned} F_{\mathrm{xj}}(\phi) &= \frac{K_t f_t R}{4\tan\beta}[-\cos 2\phi_j + K_r(2\phi_j(\mathrm{z}) - \sin 2\phi_j(\mathrm{z}))]_{z_{jl}(\phi)}^{z_{ju}(\phi)} \\ F_{yi}(\phi) &= -\frac{K_t f_t R}{4\tan\beta}[-\cos 2\phi_j(z) - \sin 2\phi_j(z)) + K_r \cos 2\phi_j(z)]_{z_{jl}(\phi)}^{z_{ju}(\phi)} \\ F_{zj}(\phi) &= -\frac{K_a K_t f_t R}{\tan\beta}[\cos\phi_j(z)]_{z_{jl}(\phi)}^{z_{ju}(\phi)} \end{aligned} \quad (5)$$

where the Z_{jl} (ϕ) and Z_{ju} (ϕ) are the upper axial engagement limits of the in cut portion of the flute j. The engagement limits depend on the cutting and the tool geometries:

$$\begin{aligned} \phi_{st}(z) &= \pi\text{-}\cos^{-1}(1-\frac{w}{R}) \quad \text{(down milling)} \\ \phi_{ex}(z) &= \cos^{-1}(1-\frac{w}{R}) \quad \text{(up milling)} \end{aligned} \quad (6)$$

In Equation (6), note that ϕ_{ex} is always π in down milling and ϕ_{st} is ways 0 in up milling according to the convention used in Figure 1. The helical cutting edges of the tool can intersect this area in different ways resulting in different integration limits. The total milling forces can then be determined as:

$$\begin{aligned} F_x(\phi) &= \sum_{j=1}^{N} F_{xj}(\phi) \\ F_y(\phi) &= \sum_{j=1}^{N} F_{yj}(\phi) \\ F_z(\phi) &= \sum_{j=1}^{N} F_{zj}(\phi) \end{aligned} \quad (7)$$

The cutting torque and power due to the tooth j can easily be determined from Equations (1) and (3) as follows:

$$\begin{aligned} T_j(\phi) &= \frac{K_t f_t R^2}{\tan\beta}[\cos\phi]_{z_{jl}(\phi)}^{z_{ju}(\phi)} \\ P_j(\phi) &= \Omega T_j(\phi) \end{aligned} \quad (8)$$

The total torque and power due to all cutting teeth can be determined similar to the summation for the forces given in Equation (7), value of the forces, torque and power can be determined after one full revolution of the tool, i.e., ϕ: 0-2π, is simulated.

For the linear-edge force model, the forces are obtained similarly using Equation (2), and integrating within the engagement limits as follows:

$$\begin{aligned} F_{xj}(\phi) &= \frac{R}{\tan\beta}\left[K_{te}\sin\phi_j(z) - K_{ne}\cos\phi_j(z) + \frac{f_z}{4}[\mathrm{K}_{rc}(2\phi_j(z) - \sin 2\phi_j(z)) - K_{tc}\cos 2\phi_j(z)]\right]_{z_{jl}}^{z_{ju}} \\ F_{xj}(\phi) &= \frac{R}{\tan\beta}\left[-K_{te}\sin\phi_j(z) - K_{ne}\cos\phi_j(z) + \frac{f_z}{4}[\mathrm{K}_{tc}(2\phi_j(z) - \sin 2\phi_j(z)) - K_{rc}\cos 2\phi_j(z)]\right]_{z_{jl}}^{z_{ju}} \\ F_{xj}(\phi) &= \frac{R}{\tan\beta}\left[K_{ae}\phi_j(z) - f_t K_{ac}\cos\phi_j(z)\right]_{z_{jl}}^{z_{ju}} \end{aligned} \quad (9)$$

The forces given by Equation (5) and (8) can be used to predict the cutting forces for a given milling process if the milling force coefficients are known. As mentioned at the beginning of this section, in the mechanistic models the force coefficients are calibrated experimentally which is explained in the following section. In this sense, mechanics of milling approach is

more general and may reduce the number of tests significantly. In case of milling an oblique cutting model has to be employed because of helical flutes. In oblique cutting models, there are several important planes which are used to measure tool angles and write down speed and force equilibrium relations [21]. The normal plane, which is perpendicular to the cutting edge, is commonly used in the analysis. After several assumptions, and velocity and the force equilibrium equations, the following expressions are obtained for the cutting force coefficients in an oblique cutting:

$$\begin{aligned} K_{tc} &= \frac{\tau}{\sin\phi_n}\frac{\cos(\gamma_n-\alpha_n)+\tan\eta_c\sin\gamma_n\tan\beta}{c} \\ K_{rc} &= \frac{\tau}{\sin\phi_n\cos\beta}\frac{\sin(\gamma_n-\alpha_n)}{c} \\ K_{ac} &= \frac{\tau}{\sin\phi_n}\frac{\cos(\gamma_n-\alpha_n)\tan\beta-\tan\eta_c\sin\gamma_n}{c} \\ c &= \sqrt{\cos^2(\phi_n+\gamma_n-\alpha_n)+\tan^2\eta_c\sin^2\gamma_n} \end{aligned} \quad (10)$$

In Equation (10), τ is the shear stress in the shear plane, ϕ_n is the shear angle in the normal plane, β is the angle of obliquity or helix angle and η_c is the chip flow angle measured on the rake face. The chip flow angle can be solved iteratively based on the equations obtained from force and velocity relations [22, 23]. However, for simplicity, Stable's rule may also be used which states that $\eta_c \approx \beta$, γ_n and α_n are the friction angle and the rake angle in the normal plane, respectively, and are given by [24]:

$$\tan\gamma_n = \tan\gamma\cos\eta_c, \tan\alpha_n = \tan\alpha_r\cos\beta \quad (11)$$

In Equation (11), α_r is the rake angle measured in the velocity plane, which is normal to the tool axis, and γ is the friction angle on the rake face. The required data is obtained from the orthogonal cutting tests in order to reduce the number of variables, thus the number of tests, and to generate a more general database which can be used for other processes as well. The shear angle, shear stress and friction coefficient can be obtained from orthogonal cutting tests as follows [25]:

$$\begin{aligned} \tan\phi &= \frac{r\cos\alpha}{1-r\sin\alpha}; \\ \tau &= \frac{(F_p\cos\phi - F_q\sin\phi)\sin\phi}{bt}; \\ \tan\gamma &= \frac{F_q+F_p\tan\alpha}{F_p-F_q\tan\alpha} \end{aligned} \quad (12)$$

where r is the cutting ratio or the ratio of the uncut chip thickness to the chip thickness, α is the rake angle, F_p and F_q are the cutting forces in the cutting speed and the feed direction, respectively.

If the linear-edge force model is to be used then the edge cutting force components must be subtracted from the cutting forces measured in each direction using linear regression. The edge force coefficients are identified from the edge cutting forces. After some cutting tests, which are repeated for a range of cutting speeds, rake angle and uncut chip thickness, an cutting database is generated for a certain tool and work material pair. These data can then be used to determine the milling cutting force coefficients using the oblique model given by Equation (10). So, we can get the force coefficients and the milling forces predicted using this approach from Equation (1), which could be demonstrated with the milling experiment results.

3. EXPERIMENTAL PROCEDURE

To demonstrate the effectiveness of the proposed force model, cutting tests were conducted with a vertical-type CNC machining center (DMU100, DMG Co., Ltd., Germany) under different cutting conditions. The cylindrical end-milling for titanium alloy was conducted by the coated WC-Co milling tool with 3 flutes, with 10 mm diameter and 30º helix angles. TiN coating material was used for the cutter in this study (UBS4AR 16036, GESAC Co., Ltd., China). A titanium alloy (TC4) block with the dimensions of 150 mm × 150 mm × 60 mm was used in the milling experiments. The three components of cutting forces on the workpiece were measured by multi - component piezoelectric dynamometer system (Kistler 9255B, Kistler Co., Ltd., Switzerland). The force signals were processed using the charge amplifiers and recorded by a PC-based data acquisition system. Following were the milling parameters: cutting speed v = 40, 80, and 120 m/min, axial cutting deep a_p = 0.2, 0.3, 0.6, 1, 2, and 3 mm, and feed for per tooth f_t = 0.01, 0.02, and 0.05 mm/z [26].

The regions of tools where wear occurred were examined using scanning electron microscopy (SEM; HITACHI S-570, Hitachi Corporation, Japan). The distribution of element on the rake face was examined by energy dispersive X-ray (EDX) spectrometry (INCA, Oxford Instrument Corporation, UK).

4. RESULTS AND DISCUSSION

During experimentation, detailed measurements were carried on the milling force. By experiments, the empirical relationships for the cutting force in milling are as follows:

$$\begin{aligned} F_x &= e^{11.3} v_c^{-0.521} f_t^{0.660} a_p^{0.807} \\ F_y &= e^{5.89} v_c^{0.226} f_t^{0.2981} a_p^{0.613} \\ F_z &= e^{-2.11} v_c^{0.226} f_t^{0.5433} a_p^{-0.20} \end{aligned} \quad (13)$$

where, F_x is the tangential cutting force, F_y is the radial cutting force, F_z is the axial cutting force, v_c is the cutting speed, f_t is the feed for each tooth, and a_p is the

axial cutting depth. Measurements on milling force were conducted during the cutting experiments for the determination of various cutting conditions. From the results obtained, it is possible to establish the relationship between processing and tool parameters to predict the milling force [27, 28].

In the simulation, the model aims are to simulate the milling process, calculate the damage initiation and evolution in the work piece material. On this basis, the prediction of cutting forces, and stress distribution in the work piece is possible by the process. A three-dimensional model (.pat document) was developed by Unigraphics NX 8.0. Then, a FE model (.fem document) was established by FEM module of UG 8.0, which was based on Lagrangian formulation with explicit integration method and associated to the three-dimensional model.

After material properties setting and dividing of grid, a simulation model (.sim document) was developed and associated to FE model for setting of the boundary and external conditions. The overall and dimensional FEM model for milling is shown in Figure 2. Each experiment was carried out using coolant. It was assumed that the cutting was removed by the coolant. Thus there were no thermal issues to be accounted in the model. The mass and inertia affects were included in the model.

The overall dynamics were not taken into consideration in the analysis. The contact and friction parameters between the tool and work piece were influenced by several factors such as cutting speed, feed rate, and geometry and surface properties. The Coulomb friction model was used and a constant friction coefficient of value 0.5 was used in the analysis. Under different machining conditions (axial cutting depth a_p, feed for each tooth f_t, the cutting speed v_c and so on), the forces, F_x, F_y and F_z can be calculated from Equation (20), and applied to the milling cutter as shown in Figure 3. After completing calculation and post-processing analysis of cutting force, the deformation and effective stress distribution for all loads of end-milling cutting tool are shown in Figures 4 and 5. The simulation conditions were cutting speed v_c = 80 m/min, feed for each tooth f_t = 0.02 mm/z, axial cutting depth a_p = 3 mm. As shown in Figures 4 and 5, deformation has a maximum value at milling tool nose (1.451 mm) and minimum value at root of the milling tool (0.102 mm). However, the effective stress has a maximum value at one milling tool nose (11942 MPa) and minimum value at another milling tool nose (0.199 MPa). The reason for this trend in results is that milling is a discontinuous process, in which when a blade cuts into the workpiece, the other blade cannot machine, and as a consequence the effective stress is small. The effective stress of middle and bottom parts of the milling tool gradually increased to higher values than others.

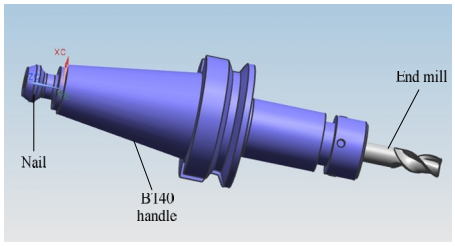

(a) Overall FEM model in milling

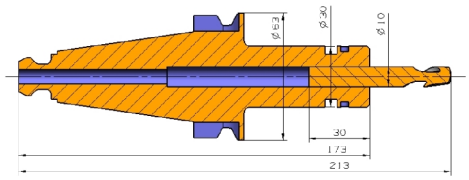

(b) Dimension of FEM model in milling

Figure 2. Overall and dimensional FEM model in milling

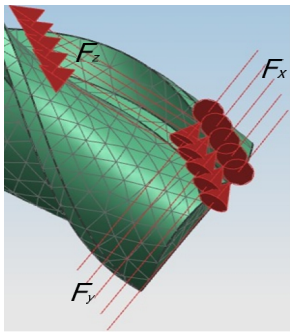

Figure 3. Loads on FEM model in milling

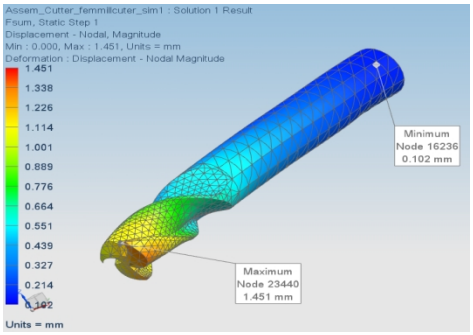

Figure 4. Deform distribution for end-milling cutting tool

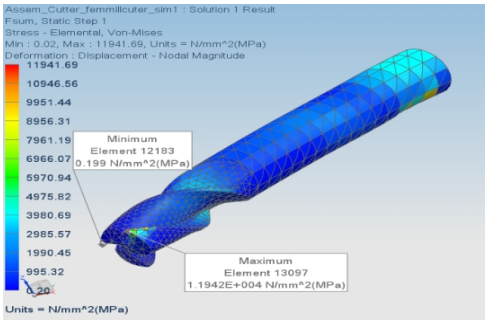

Figure 5. Effective stress distribution for end-milling cutting tool

Figure 6 illustrates the effect of axial cutting depth on maximum deformation and effective stress for all loads of end-milling cutting tool. It can be seen that when the axial cutting depth is 0.2 mm, the maximum deformation and effective stress are only 0.08 mm and 2360 MPa, respectively. However, when the axial cutting depth increased to 3.0 mm, the maximum deformation and effective stress respectively increased to 1.451 mm and 11942 MPa. This indicates that the maximum deformation and effective stress have an upward trend for machining of end-milling cutting tool.

The implementation of cutting process simulation is based on numerical theory and techniques. Their development will be helpful to improve the capability of simulation. The adaptive meshing technique which is used in the finite element method is accomplished using R-adaptively. During this adaptive application, the meshing nodes are moved to more favorable positions to reduce mesh distortion. From the above methodology, expression for the resultant cutting force F_N, was obtained as:

$$F_N = e^{8.46} v_c^{0.0395} f_t^{0.598} a_p^{0.85} \quad (14)$$

After completing calculation and post-processing analysis of the resultant cutting force F_N, from Equation (14). During the experiment it was found that there were some damages at the nose of milling tool while machining the aluminum alloy for 30 min at a speed of 80 m/min, feed for each tooth f_t = 0.02 mm/z, and axial cutting depth a_p = 3 mm.

The SEM micrograph and EDX spectral diagram of the fractured area of milling tool nose are shown in Figure 7. After ultrasonic cleaning, transfer of Al element from it to cutting tool surface was not observed. However, elements, such as Mo, Ni and Ta which are difficult to clean remained on the surface.

The No. 1 area is the cutting tool substrate without the coating in fracture zone. From Figure 7 (b), it can be seen that the main materials of tool matrix are WC, and Co. In Figure 7 (c), the No. 2 area is mainly the junction of the coating and substrate. Because the intensity of Ti peak is higher than that of W peak No. 3 area is the unworn coated area. In the other words, the content of TiN film is higher than that of WC matrix.

The efficiency, E for milling of titanium alloy can be expressed as:

$$E = 1000v \cdot a_p \cdot f_t \quad (15)$$

The units for E are mm^3/min. The graphical relationship based on the empirical Equation (14) of the cutting force of tool and the results of cutting efficiency calculated using Equation (15) are shown in Figure 8. The solid line represents the equivalent efficiency and the dotted line is the equivalent cutting force. The fitting condition is for the feed rate of f_t= 0.02 mm/r.

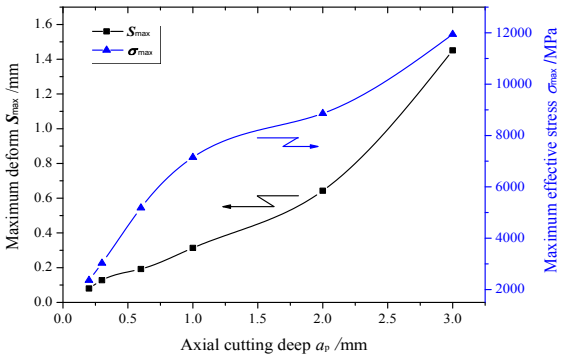

Figure 6. Effect of axial cutting depth on the maximum deformation and effective stress for all loads of end-milling cutting tool

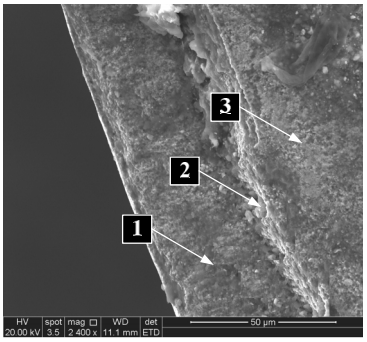

(a) SEM micrograph of the wear area of carbide coating tool

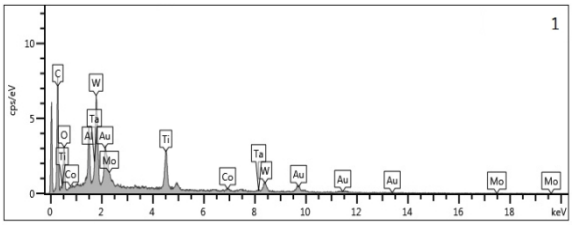

(b) EDX spectrum diagram of point scanning for No. 1 area

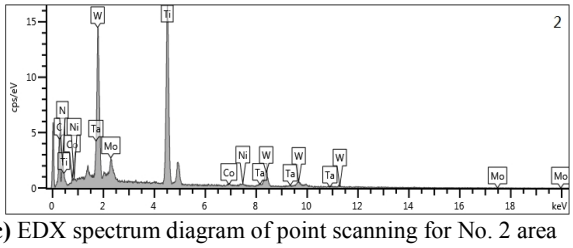

(c) EDX spectrum diagram of point scanning for No. 2 area

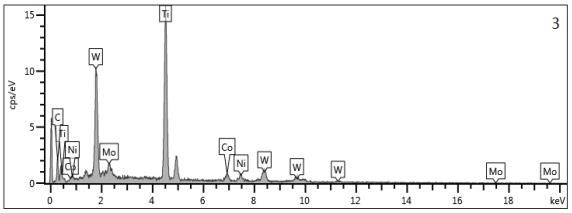

(d) EDX spectrum diagram of point scanning for No. 3 area

Figure 7. SEM micrograph and EDX spectra of the fracture area of milling tool nose

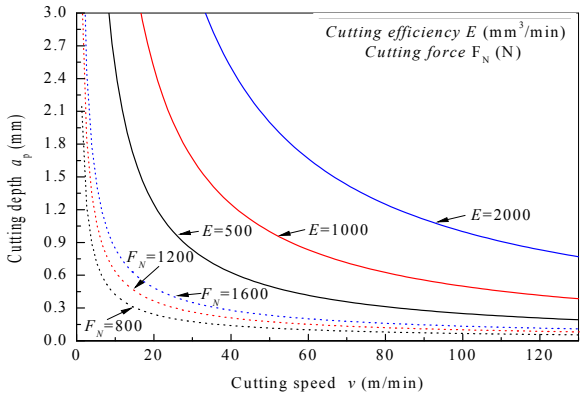

Figure 8. Efficiency-cutting force curve for machining titanium alloy

As can be seen from Figure 8, a good cutting effect is obtained by increasing the cutting speed and decreasing the cutting depth at constant efficiency. A reasonable cutting efficiency of the tool is E=1000 mm^3/min. For the semi-finished machining of the titanium alloy with a TiN coated cemented carbide milling tool, following cutting parameters are recommended: cutting speed (v) of 80~100 m/min; cutting depth of 0.6~2 mm; and feed rate of 0.01~0.02 mm/r. A cutting efficiency of the tool, E=1000 mm^{3}min for the recommended cutting parameters should be expected as reasonable.

5. CONCLUSIONS

The experiment was made for the milling of titanium alloy by coated cemented carbide cutting tool. Based on the cutting force theory, the cutting forces can be predicted satisfactorily with simulation of the end milling by finite element method. Following reasons may be attributed for higher accuracy of simulation results compared to that obtained with theoretical relationships:

1. The mechanistic force models were introduced in force predictions for most applications. Material properties in the simulations were defined based on the cutting force theory, as they were a function of strain and strain rate whereas in the theoretical relationships, the properties were simply kept constant.
2. When the axial cutting depth was 0.2 mm, the maximum deformation and effective stresses respectively were only 0.08 mm and 2360 MPa. However, when the axial cutting depth was increased to 3.0 mm, the maximum deformation and effective stress increased to 1.451 mm and 11942 MPa, respectively, indicating that the maximum deformation and effective stress showed an upward trend for machining of end-milling cutting tool.
3. A good cutting effect is obtained by increasing the cutting speed and decreasing the cutting depth at constant efficiency. The reasonable cutting parameters obtained from the analyses of the cutting efficiency and cutting force of the tools were as follows: cutting speed (v) of 80~100 m/min; cutting depth of 0.6~2 mm; and feed rate of 0.01~0.02 mm/r.

6. ACKNOWLEDGMENT

This work was supported by National Natural Science Foundation of China (No. 51475222), the Science and Technology Development Foundation of Henan Province (No. 132102210514), the Outstanding Youth Innovation Foundation for Science and Technology of Henan province (No. 144100510017), the International Cooperation Projects for Science and Technology of Henan province (No. 144300510050), the Young Backbone Teachers Foundation for the Universities of Henan Province (No. 2013GGJS-186) and the Development Program for Science and Technology of Luoyang (No. 1202016A).

7. REFERENCES

1. Kline W. A., and DeVor R., "The effect of runout on cutting geometry and forces in end milling", ***International Journal of Machine Tool Design and Research***, Vol. 23, No. 2, (1983), 123-140.
2. Dombovari Z., Munoa J., and Stepan G., "General Milling Stability Model for Cylindrical Tools", ***Procedia CIRP***, Vol. 4, No. 0, (2012), 90-97.
3. Zaghbani I., and Songmene V., "Estimation of machine-tool dynamic parameters during machining operation through operational modal analysis", ***International Journal of Machine Tools and Manufacture***, Vol. 49, No. 12–13, (2009), 947-957.
4. Wan M., Wang Y.-T., Zhang W.-H., Yang Y., and Dang J.-W., "Prediction of chatter stability for multiple-delay milling system under different cutting force models", ***International Journal of Machine Tools and Manufacture***, Vol. 51, No. 4, (2011), 281-295.
5. Thomas M., and Beauchamp Y., "Statistical investigation of modal parameters of cutting tools in dry turning", ***International Journal of Machine Tools and Manufacture***, Vol. 43, No. 11, (2003), 1093-1106.
6. Li H. Z., Zhang W. B., and Li X. P., "Modelling of cutting forces in helical end milling using a predictive machining theory", ***International Journal of Mechanical Sciences***, Vol. 43, No. 8, (2001), 1711-1730.
7. Smith S., and Tlusty J., "An overview of modeling and simulation of the milling process", ***Journal of Engineering for Industry(Transactions of the ASME)***, Vol. 113, No. 2, (1991), 169-175.
8. Budak E., and Altintas Y., "Modeling and avoidance of static form errors in peripheral milling of plates", ***International***

Journal of Machine Tools and Manufacture, Vol. 35, No. 3, (1995), 459-476.

9. SadeghpourHaji M., Mirbagheri S., Javid A., Khezri M., and Najafpourd G., "A Wavelet Support Vector Machine Combination Model for Daily Suspended Sediment Forecasting", ***International Journal of Engineering Transaction B: Applications***, Vol. 27, No. 6, (2014), 855-864.
10. Sadeghi M., Naserian R. S., and Haghighat H., "An instantaneous rigid force model for 3-axis ball-end milling of sculptured surfaces", ***International Journal of Engineering Transaction B: Applications***, Vol. 16, No. 4, (2003), 385-394.
11. Özel T., and Altan T., "Process simulation using finite element method — prediction of cutting forces, tool stresses and temperatures in high-speed flat end milling", ***International Journal of Machine Tools and Manufacture***, Vol. 40, No. 5, (2000), 713-738.
12. Budak E., and Altintas Y., "Analytical prediction of chatter stability in milling-Part II: Application of the general formulation to common milling systems", ***Journal of dynamic systems, measurement, and control***, Vol. 120, No. 1, (1998), 31-36.
13. Davies M., Pratt J., Dutterer B., and Burns T., "The stability of low radial immersion milling", ***CIRP Annals-Manufacturing Technology***, Vol. 49, No. 1, (2000), 37-40.
14. Campa F. J., Lopez de Lacalle L. N., and Celaya A., "Chatter avoidance in the milling of thin floors with bull-nose end mills: Model and stability diagrams", ***International Journal of Machine Tools and Manufacture***, Vol. 51, No. 1, (2011), 43-53.
15. Li X. P., and Li H. Z., "Theoretical modelling of cutting forces in helical end milling with cutter runout", ***International Journal of Mechanical Sciences***, Vol. 46, No. 9, (2004), 1399-1414.
16. Altintas Y., Spence A., and Tlusty J., "End milling force algorithms for CAD systems", ***CIRP Annals-Manufacturing Technology***, Vol. 40, No. 1, (1991), 31-34.
17. Weck M., Altintas Y., and Beer C., "CAD assisted chatter-free NC tool path generation in milling", ***International Journal of Machine Tools and Manufacture***, Vol. 34, No. 6, (1994), 879-891.
18. Budak E., Altintas Y., and Armarego E., "Prediction of milling force coefficients from orthogonal cutting data", ***Journal of Engineering for Industry***, Vol. 118, No. 2, (1996), 216-224.
19. Maurel-Pantel A., Fontaine M., Thibaud S., and Gelin J. C., "3D FEM simulations of shoulder milling operations on a 304L stainless steel", ***Simulation Modelling Practice and Theory***, Vol. 22, No. 0, (2012), 13-27.
20. Pittalà G. M., and Monno M., "A new approach to the prediction of temperature of the workpiece of face milling operations of Ti-6Al-4V", ***Applied Thermal Engineering***, Vol. 31, No. 2–3, (2011), 173-180.
21. Rantatalo M., Aidanpää J.-O., Göransson B., and Norman P., "Milling machine spindle analysis using FEM and non-contact spindle excitation and response measurement", ***International Journal of Machine Tools and Manufacture***, Vol. 47, No. 7–8, (2007), 1034-1045.
22. EL-Desouky A. R., and EL-Wazery M. S., "Mixed Mode Crack Propagation of Zirconia/Nickel Functionally Graded Materials", ***International Journal of Engineering, Transaction B: Applications***, Vol. 26, No. 8, (2013), 885-894.
23. Li J. L., Jing L. L., and Chen M., "An FEM study on residual stresses induced by high-speed end-milling of hardened steel SKD11", ***Journal of Materials Processing Technology***, Vol. 209, No. 9, (2009), 4515-4520.
24. Engin S., and Altintas Y., "Mechanics and dynamics of general milling cutters.: Part ii: inserted cutters", ***International Journal of Machine Tools and Manufacture***, Vol. 41, No. 15, (2001), 2213-2231.
25. Liwen G., Chunxia Z., Huifeng Z., and Huayang X., "Modeling and Analysis of a Super Heavy Numeric Control Boring and Milling Machine", ***IERI Procedia***, Vol. 1, No. 0, (2012), 199-204.
26. Sun J., and Guo Y. B., "A new multi-view approach to characterize 3D chip morphology and properties in end milling titanium Ti-6Al-4V", ***International Journal of Machine Tools and Manufacture***, Vol. 48, No. 12-13, (2008), 1486-1494.
27. Sadegheih A., and Drake P., "A novel experimental analysis of the minimum cost flow problem", ***International Journal of Engineering Transaction A: Basics***, Vol. 22, No. 3, (2009), 251-268.
28. Fallahnezhad M., Sajjadieh M., and Abdollahi P., "An Iterative Decision Rule to Minimize Cost of Acceptance Sampling Plan in Machine Replacement Problem", ***International Journal of Engineering Transaction A: Basics***, Vol. 27, No. 7, (2014), 1099-1106.

Modelling and Numerical Simulation of Cutting Stress in End Milling of Titanium Alloy using Carbide Coated Tool

B. Li[a], Y. Wang[b], H. Li[a], H. You[a]

[a]*School of Mechanical Engineering, Luoyang Institute of Science and Technology, Luoyang 471023, Henan Province, PR China*
[b]*School of Environmental Engineering and Chemistry, Luoyang Institute of Science and Technology, Luoyang 471023, Henan Province, PR China*

P A P E R I N F O

Paper history:
Received 19 April 2015
Received in revised form 25 May 2015
Accepted 11 June 2015

Keywords:
Finite Element Modeling
End-milling
Cutting Force
Simulation

چکیده

مدل های نیروی مکانیکی در پیش بینی های نیروی دقت بالا برای اکثر برنامه های کاربردی معرفی شدند. آزمایشی برای فرز آلیاژ تیتانیوم توسط ابزار برش کاربید سمان پوشش داده شده انجام شد. بر اساس نظریه نیروی برش، نتایج آزمایش ها و روش المان محدود، ما می توانیم به رابطه نیروی برش به صورت دقیق دست یابیم، که می تواند به یک پایگاه داده بزرگ برش توسعه داده شود. با توجه به تجزیه و تحلیل، حداکثر تغییر شکل و تنش موثر نشان دهنده روند افزایش برای ماشینکاری با ابزار برش فرز پایانی بود. مجموعه ای مناسب از پارامترهای فرز برای ماشینکاری آلیاژ تیتانیوم توسط ابزار برش کاربید سمان پوشش داده شده از طریق تجزیه و تحلیل بهره وری برش در رابطه با نیروی برش ابزارها به دست آمد. انتظار می رود که این مطالعه مبنایی پایه ای برای بهینه سازی پارامترهای برش برای آلیاژ تیتانیوم ارائه کند.

***doi**: 10.5829/idosi.ije.2015.28.07a.16*